Geoscientific
Model Development
Discussions

Open Access

Development of PM$_{2.5}$ source impact spatial fields using a hybrid source apportionment air quality model

C. E. Ivey[1], H. A. Holmes[2], Y. T. Hu[1], J. A. Mulholland[1], and A. G. Russell[1]

[1]Georgia Institute of Technology, Atlanta, Georgia, USA
[2]University of Nevada Reno, Reno, Nevada, USA

Correspondence to: C. E. Ivey (sunni.ivey@gmail.com)

GMDD

8, 645–671, 2015

Development of PM$_{2.5}$ source impact spatial fields

C. E. Ivey et al.

Title Page

Abstract	Introduction
Conclusions	References
Tables	Figures

Back | Close

Full Screen / Esc

Printer-friendly Version

Interactive Discussion

Abstract

An integral part of air quality management is knowledge of the impact of pollutant sources on ambient concentrations of particulate matter (PM). There is also a growing desire to directly use source impact estimates in health studies; however, source impacts cannot be directly measured. Several limitations are inherent in most source apportionment methods, which has led to the development of a novel hybrid approach that is used to estimate source impacts by combining the capabilities of receptor modeling (RM) and chemical transport modeling (CTM). The hybrid CTM-RM method calculates adjustment factors to refine the CTM-estimated impact of sources at monitoring sites using pollutant species observations and the results of CTM sensitivity analyses, though it does not directly generate spatial source impact fields. The CTM used here is the Community Multi-Scale Air Quality (CMAQ) model, and the RM approach is based on the Chemical Mass Balance model. This work presents a method that utilizes kriging to spatially interpolate source-specific impact adjustment factors to generate revised CTM source impact fields from the CTM-RM method results, and is applied to January 2004 over the continental United States. The kriging step is evaluated using data withholding and by comparing results to data from alternative networks. Directly applied and spatially interpolated hybrid adjustment factors at withheld monitors had a correlation coefficient of 0.89, a linear regression slope of 0.83 ± 0.02, and an intercept of 0.14 ± 0.02. Refined source contributions reflect current knowledge of PM emissions (e.g., significant differences in biomass burning impact fields). Concentrations of 19 species and total PM$_{2.5}$ mass were reconstructed for withheld monitors using directly applied and spatially interpolated hybrid adjustment factors. The mean concentrations of total PM$_{2.5}$ for withheld monitors were 11.7($\pm$8.3), 16.3($\pm$11), 8.59($\pm$4.7), and 9.20($\pm$5.7) μg m^{-3} for the observations, CTM, directly applied hybrid, and spatially interpolated hybrid predictions, respectively. Results demonstrate that the hybrid method along with a spatial extension can be used for large-scale, spatially resolved source apportionment studies where observational data are spatially and temporally

limited. Data withholding also provides an estimate of method uncertainty. Species concentrations were reconstructed using spatial hybrid results, and the error relative to observed concentrations was greatly reduced as compared to CTM-simulated concentrations.

1 Introduction

Variations in ambient pollutant species concentrations, including particulate matter (PM) and gases, are correlated with health outcomes such as lower birth weight (Darrow et al., 2011; Wang et al., 1997), higher occurrences of bradycardia and central apnea (Campen et al., 2001; Peel et al., 2011); decreased peak expiratory flows and increased respiratory symptoms in non-smoking asthmatics (Peters et al., 1997); and all-cause, lung cancer, and cardiopulmonary mortality (Pope et al., 2002). Additionally, nanotoxicological studies report that particle uptake by cells and entry into blood and lymph leads to oxidative stress in sensitive areas of the body such as lymph nodes, bone marrow, and the spleen (Oberdorster et al., 2005). Recently, in a study on the global burden of disease, of the 67 risk factors studied, exposure to ambient particulate matter pollution was the ninth highest risk factor leading to disability-adjusted life years (Lim et al., 2012). Many past epidemiological studies focused on associating PM mass (e.g., $PM_{2.5/10}$: PM with aerodynamic diameters less than 2.5 or 10 µm) with the health outcomes, as opposed to individual species or the sources of the PM due to limited data availability or difficulties in quantifying source impacts. Epidemiological studies are examining the associations between individual species and health outcomes using data from ground observation networks, such as the Chemical Speciation Network (CSN) and the Southeastern Aerosol Research and Characterization Network (SEARCH) (Dominici et al., 2010; Samet et al., 2000; Sarnat et al., 2008; Tolbert et al., 2007). It is of further interest to determine the degree to which individual sources are influencing health events and to link human exposure and subsequent adverse impacts to sources and multi-pollutant mixtures (Laden et al., 2000; Thurston

et al., 2005). Attributing individual component concentrations and the overall mixture of observed air pollution to specific sources, and then linking those sources with adverse health impacts is challenging. Typically, receptor modeling (RM) is used to generate source apportionment (SA) results for epidemiological studies because longer time se-
5   ries are required (e.g., greater than two years) (Sarnat et al., 2008).

Several SA models have been developed to quantify source impacts on pollutant concentrations. Each model has its own unique characteristics and associated uncertainties (Balachandran et al., 2012; Seigneur et al., 2000). In an effort to improve the spatial and temporal resolution of SA data, chemical transport models (CTM) have
10 been adapted to estimate emission impacts on pollutant concentrations. This work utilizes a hybrid CTM-RM method to provide spatial fields of source impacts for use in detailed health-related, spatiotemporal analyses (e.g., Sarnat et al., 2008).

The goal of this study is to create spatial fields of source impacts by spatially interpolating source impact adjustment factors (ratios, or R's) and then applying those
15 adjustments to CTM source impact fields. R's are generated by a hybrid CTM-RM SA approach that integrates observational data and results from a CTM to calculate an emission-based adjustment of source impacts at receptor locations (Hu et al., 2014). Kriging is employed to generate spatial fields of R's for 33 emissions sources. The spatial fields of adjustment factors are applied to original source impact fields to produce
20 hybrid-adjusted source impact and species concentration fields for the continental US. The adjustments can also be interpolated in time to adjust source impact fields on days when speciated observations are not available. The performance of the spatial extension is evaluated by performing data withholding and by comparing results to observations from other monitoring networks. The hybrid CTM-RM method, along with
25 the spatial extension, provides air quality data fields for health studies that require spatially-resolved exposure metrics. This approach can also be used to assist air quality planners in developing state implementation plans (SIPs) and assessing exceptional events, such as wildland fires.

2 Data and methods

2.1 Data

Observational data during January 2004 from 189 monitors in the Chemical Speciation Network (CSN) were used for model development and evaluation (Fig. 1). Data were obtained on one in every three or six days in January 2004 for a total of 9 days (e.g., 4, 7, 10...28 January), which led to varying sample sizes for each observation day. CSN monitor measurements include total PM$_{2.5}$, organic and elemental carbon, ions, and 35 metals. CSN monitors tend to be located in more densely populated areas such as urban and suburban areas, and data are more associated with high-population emissions sources such as mobile and cooking sources. Speciated PM$_{2.5}$ data are also available from the SEARCH (Hansen et al., 2003, 2006) and IMPROVE (Chow et al., 1993) networks, and those data were used for further model evaluation. The SEARCH network includes eight monitors in the southeastern US, configured as urban/rural pairs. IMPROVE monitors are mainly located in pristine locations such as national parks and wilderness areas. Thirty-eight IMPROVE monitors in the eastern US were used for model evaluation. Monitors in the eastern US were used due to their closer proximity with urban monitoring sites (e.g., less than 50 km), as opposed to western IMPROVE sites which are much more spatially sparse. Additionally, modeled processes have higher uncertainty for the western US due to complex terrain and meteorology, leading to added bias in the observation and model comparison (Baker et al., 2011).

2.2 CTM-RM hybrid method

This study utilizes a hybrid SA method that combines techniques of both CTMs and RMs to generate adjustment factors (symbolized by R) that improve source impact estimates. Hu et al. (2014) describe the hybrid approach in detail, but it is briefly summarized here. First, gridded concentrations and emissions sensitivities of PM$_{2.5}$

species are generated using CMAQ-DDM (CMAQ v. 4.7 or 5.0.2) (Byun and Schere, 2006; Dunker, 1981, 1984; Napelenok et al., 2006) with traditional inputs for emissions (Sparse Matrix Operator Kernel Emissions, SMOKE, CEP, 2003), meteorology (Fifth-Generation PSU/NCAR Mesoscale Model, MM5, Grell et al., 1994), and terrain (Pleim and Xiu, 1995; Xiu and Pleim, 2001). CMAQ-DDM model sensitivities to emissions are designated as the original (base case) source impacts ($SA_{i,j}^{base}$) for species i and source j. Next, the original source impacts, receptor observations, and uncertainties are used as inputs to the objective function (Eq. 1) of the hybrid SA model.

$$X^2 = \sum_{i=1}^{N} \left[\frac{\left[\left(c_i^{obs} - c_i^{sim} \right) - \sum_{j=1}^{J} SA_{i,j}^{base} (R_j - 1) \right]^2}{\sigma_{i,obs}^2 + \sigma_{i,SP}^2} \right] + \Gamma \sum_{j=1}^{J} \frac{\ln(R_j)^2}{\sigma_{\ln(R_j)^2}} \tag{1}$$

where the adjustment factors R_j are optimized by minimizing the objective function, χ^2. The terms c_i^{obs} and c_i^{sim} represent the observed and CMAQ-simulated concentrations, respectively; Γ weights the amount of change in source impact. Uncertainties in observation measurement ($\sigma_{i,obs}$), source profiles ($\sigma_{i,SP}$), and source strength ($\sigma_{\ln(R_j)}$) are also included in the model. The objective function is minimized by using a nonlinear optimization approach known as sequential quadratic programming (Fletcher, 1987; Gill et al., 1981). The function is modeled using a ridge regression structure, as demonstrated by the second term, and uses an effective variance approach to balance model outputs (Watson et al., 1984).

Source profiles are derived from the information provided by Reff et al. (2009). Uncertainties in the first term of the objective function serve as effective variances of the numerator and are specified for each species i. Finally, R_j are applied to $SA_{i,j}^{base}$ to adjust original source impact estimates (Eq. 2) and reconstruct simulated concentrations

Full Screen / Esc

Printer-friendly Version

Interactive Discussion

(c_i^{adj}) at receptors to more closely reflect observations (Eq. 3).

$$SA_{i,j}^{adj} = R_j SA_{i,j}^{base} \tag{2}$$

$$c_i^{adj} = c_i^{sim} + \sum_{j=1}^{J} SA_{i,j}^{base}(R_j - 1) \tag{3}$$

Given that many of the source profiles are similar between categories such that colin-
earities are present, the variation of the R_j's are constrained to $0.1 \leq R_j \leq 10$.

The hybrid CTM-RM method produces results that more closely reflect observations
than the original CTM results, which are often biased (Hu et al., 2014). It accounts for
more known source categories than traditional RM approaches (e.g., 33 vs. 6), and it
links sources and observations both temporally and spatially. Additionally, the hybrid
CTM-RM method generates estimates of the uncertainty in source impact predictions
and identifies potential errors in source strength and composition. One limitation of the
hybrid CTM-RM method is that results are only available at receptor locations when
observations are available, limiting its spatial and temporal scope. In this paper, the
spatial hybrid method is presented and evaluated, and it extends the benefits of the
hybrid CTM-RM method through spatial interpolation.

2.3 Development of spatiotemporal fields

Spatial and temporal source impact fields can be developed by combining the hybrid
CTM-RM method and geostatistical techniques (see Fig. S1 in the Supplement for
a flow diagram of the methods). Hybrid-generated R_j were spatially interpolated for
each observation day using kriging to generate spatial fields of source impact adjust-
ment factors. Matlab© (v. 7.14.0.739) was used to perform all geostatistical and opti-
mization calculations.

Daily-averaged spatial fields of CMAQ-DDM source impacts are adjusted by grid-
by-grid multiplication of the original fields by the corresponding adjustment factor field,

Title Page

Abstract | Introduction

Conclusions | References

Tables | Figures

|◄ | ►|

◄ | ►

Back | Close

Full Screen / Esc

Printer-friendly Version

Interactive Discussion

resulting in spatial fields of hybrid-adjusted source impacts that are available every third day, as are observations. In later work, source impact fields for intervening periods are developed by interpolation of the R_j's. Temporally interpolating R_j and then applying those adjustments to simulated source impact fields is preferred over simply interpolating the 1-in-3 day hybrid-adjusted source impact fields because temporally interpolating adjusted source impacts would smooth the fields and the day-specific spatial and temporal variability in the emissions and meteorology captured by the CTM would be lost.

2.4 Method evaluation

Performance of the spatial extension was evaluated using a data withholding approach for which 10 % of CSN monitors with associated hybrid data were randomly removed from the data set for each observation day ($N = 75$ total removed points). The remaining 90 % were used to fit the variogram models used for kriging to produce spatial fields of R_j. Spatially interpolated R_j values were extracted for grids containing the withheld monitors. The hybrid optimization is directly applied to withheld receptors to assess the performance of the kriging model. Concentrations are reconstructed using Eq. (3) and the spatially interpolated adjustment factors. Finally, the original CMAQ-DDM, directly applied hybrid (CTM-RM), and spatial hybrid (SH) concentrations are compared to observed concentrations at withheld receptors. Linear regression was used to assess correlations between observations and modeled concentrations. Results were also evaluated at SEARCH and IMPROVE locations, where CMAQ-DDM and hybrid concentrations were compared to observations. Note that the application of the hybrid method, as conducted here, did not include SEARCH and IMPROVE data, and CTM-RM/SH results are independent of those observation data. Also note that 41 species, including total PM, were used for spatial field construction, but only results for 20 species are presented for comparison of CSN results and 15 species for SEARCH and IMPROVE results, as measurements for some trace metals are seldom above measurement detection limit.

Full Screen / Esc

3 Results

3.1 Hybrid adjustment factors

After application of the hybrid CTM-RM method at each of the monitors and spatial extension over the continental US, it was found that while many of the source impacts were adjusted relatively little (i.e., $R \approx 1.0$), dust- and biomass burning-related impacts were often biased high in the original CMAQ-DDM simulation and therefore considerably reduced. Spatial fields of hybrid adjustment factors are presented for dust, on-road diesel and gasoline combustion, and woodstove sources (Fig. 3); mean and median values for R_j's for all sources are presented in the Supplement (Table S2) as well as source-specific probability distribution functions (Fig. S3). Typically, R_j's were less than one for dust and woodstove impacts, indicating a high bias in those source impacts in the base CMAQ-DDM simulations. Spatial field values for on-road diesel and gasoline combustion R_j's are generally near one over most of the US, though R_j's for those sources tend be below one in the southeastern region of the US. The distribution of all R_j values was approximately lognormal, and an analysis was performed to determine whether log-transformation of R_j prior to the kriging step was necessary to reduce bias in source impact and concentration estimates. From the analysis it was determined that lognormal transformation of R_j values was not necessary, as little difference was observed in reconstructed concentrations and source impact fields as a result of the transformation.

3.2 Refined spatial fields

Base CMAQ-DDM spatial fields were refined by applying kriged fields of hybrid adjustment factors (Fig. 2). Sources with high occurrences ($\sim > 50\%$) of adjustment factors less than 1 include biomass burning, metals processing, and natural gas combustion; refined spatial fields are presented in the Supplement (Figs. S5–S7). Biomass burning includes impacts from agricultural burning, lawn waste burning, open fires, prescribed

burning, wildfires, woodfuel burning, and woodstoves. The SH method significantly decreases impacts from biomass burning on 4 and 22 January for the eastern US and for portions of the west coast (Fig. S5), largely driven by the observed potassium and OC levels being lower than simulated levels. On average, CMAQ-DDM simulated levels were a factor of 3.1 ± 1.1 times higher than SH values on 4 January, and a factor of 5.2 ± 1.0 times higher on 22 January. Metal processing impacts were reduced for areas highly impacted by smelting and metal works industries including the Ohio River Valley and Mid-Atlantic regions. On average, the base simulated values were $21 \pm 21\%$ higher than SH values on 4 January, and $25 \pm 21\%$ higher on 22 January for metal processing impacts. Natural gas combustion source impacts (area and point sources only) were reduced for the southeastern US, the Ohio River Valley Region, the Gulf Coast states, and parts of California and Texas. On average, simulated levels were $35 \pm 14\%$ higher than SH values on 4 January, and $72 \pm 28\%$ higher on 22 January for natural gas combustion impacts.

3.3 Refined source impacts

Average source contributions to $PM_{2.5}$ at withheld CSN monitors were ranked from largest to smallest for the base CMAQ-DDM (without any adjustment), directly applied hybrid (CTM-RM, available at the monitors), and interpolated spatial hybrid (SH) results (Table 1). The top three sources were woodstoves, dust, and livestock emissions for base CMAQ-DDM simulations, the latter capturing the influence of ammonia emissions on the formation of nitrate. The livestock category includes impacts from other agricultural/farming activities. For CTM-RM and SH results, woodstove (10th for both) and dust (13th for CTM-RM, 14th for SH) were ranked much lower. Livestock emissions were ranked 1st for both the CTM-RM and SH hybrid applications. Source ranking for open fires was reduced from 10th (CMAQ-DDM) to 20th for both the CTM-RM and SH applications. The fuel oil source impact ranking increased from 12th for the base CMAQ-DDM simulation to 6th and 5th for CTM-RM and SH results, respectively.

3.4 Refined concentration estimates

In the method evaluation, 10 % of the CSN monitors were withheld, and source impacts were calculated at the monitor location using the SH method for comparison to the observed species concentrations. The mean concentrations of total $PM_{2.5}$ for withheld monitors were 11.7($\pm$8.3), 16.3($\pm$11), 8.59($\pm$4.7), and 9.2($\pm$5.7) µg m^{-3} for the observations, CMAQ-DDM, CTM-RM, and SH estimations, respectively. Levels of crustal metals (Al, Ca, Fe, and Si), K, and Cl were biased very high in the base CMAQ-DDM simulation, oftentimes an order of magnitude greater than observations. SH concentrations of metals were closer to the CSN observations. Error in simulated (sim) concentrations is calculated using Eq. (4):

$$\text{Error} = \sum_{i=1}^{N} \frac{|\text{obs}_i - \text{sim}_i|}{\text{obs}_i} \tag{4}$$

For example, the error was 295 and 139 % for CMAQ-DDM vs. observations and SH vs. observations, respectively for vanadium; and 1340 and 326 % for CMAQ-DDM vs. observations and SH vs. observations, respectively for manganese. Mean observed and modeled concentrations for total PM mass, five major species, and other metals can be found in the Supplement (Table S3).

3.5 Spatial extension evaluation

CTM-RM and SH species concentrations and adjustment factors at withheld monitors were compared to evaluate the spatial interpolation that was performed using kriging. For each observation day (9 days), 10 % of available monitors were randomly withheld, resulting in a total of 2475 data pairs (75 withheld sites × 33 source categories). Five outlying data pairs (< 0.5 %) were removed from this regression ($R_{\text{Hyb}} > 2$). The remaining CTM-RM and SH factors had a Pearson correlation coefficient of 0.89, a linear

regression slope of 0.83 ± 0.02, and an intercept of 0.14 ± 0.02 (Fig. 4). Root mean square errors (RMSE) were calculated for the adjustment factors by source (Eq. 5):

$$\text{RMSE}_j = \sqrt{\frac{\sum_{i=1}^{N} \left(R_j^{\text{CTM-RM}} - R_j^{\text{SH}} \right)^2}{N}}, \qquad j = 1 \ldots J \text{ sources}, \ N = 75 \text{ sites} \qquad (5)$$

RMSEs for all sources were less than 0.4, with the exception of RMSEs for lawn waste burning, prescribed burning, and woodstoves (Table S2). This is expected given the uncertainty in the burn emissions. Mean and median R_j's for each source are also calculated, and values are within 20 % for most source (Table S2). The overall mean R_j at withheld monitors for all sources for CTM-RM and SH adjustment factors was 0.84 and 0.83 respectively, indicating a high bias in CMAQ-DDM overall, as expected from the base model performance evaluation (PM$_{2.5}$ was biased approximately 40 % high).

Probability distributions were examined for CTM-RM and SH adjustment factors for each source (Fig. S3). Cumulative distributions of adjustment factors were highly correlated for each source. The spatial interpolation captured CTM-RM trends for sources dominated by adjustment factors near 0.1, such as dust, lawn waste burning, prescribed burning, and woodstoves, though did not capture all of the extremely low adjustments (e.g., meat cooking in some locations). Sources that found little adjustment ($R_j = 1$) include aircraft, diesel combustion (stationary sources), fuel oil burning, Mexican combustion, non-road liquid petroleum gasoline combustion, and seasalt, and were well captured by the spatial extension, as demostrated by nearly identical PDFs.

3.6 SEARCH and IMPROVE comparison

The spatial extension of the hybrid method was further evaluated by comparing simulated concentrations to independent data from the SEARCH and IMPROVE networks (Tables S4–S5 and S7–S8). The mean concentrations over observation days were compared, as well as regression statistics for observations vs. modeled results. For

the SEARCH network ($N = 8$), 15 species were compared to observations. Error in mean concentrations for crustal elements was significantly decreased (CMAQ-DDM and SH): Al, 2203 to 540 %; Si, 1228 to 271 %; K, 365 to 61 %; Ca, 402 to 61 %; Fe, 260 to 3 %; Cu, 231 to 38 %; and Se, 63 to 25 %. For the IMPROVE network ($N = 38$), errors in mean concentrations for crustal elements were also significantly decreased: Al, 704 to 24 %; Si, 371 to 24 %; K, 599 to 48 %; Ca, 361 to 36 %; Fe, 334 to 18 %; Cu, 186 to 57 %; and Se, 22 to 11 %. The large remaining errors stem from the source profiles leading to some elements being biased consistently high, others low. Further work to optimize source profiles can reduce residual errors.

4   Discussion

CTM-RM and SH adjustment factors are well-correlated for each source category for withheld monitors. Kriging captures the original distributions of adjustment factors for each source as simulated by the CTM-RM analysis. Spatial interpolation of hybrid adjustment factors is well-suited for providing spatial fields of refined source impacts for multiple distinct source categories. Kriged adjustment factors also provide refined source contribution estimates that are more consistent with observations than CMAQ-DDM.

The order of source contributions at withheld monitors for the CTM-RM and SH applications compared well when ranked by magnitude in descending order, though often differed greatly from the base CMAQ-DDM application. The difference in rankings between CTM-RM and SH contributions was, at most, 2 positions. The top three sources of primary PM$_{2.5}$ for January 2004, based on source emissions, were dust, woodstoves, and coal combustion, estimated at 1275, 5301, and 3407 metric tons per day, respectively (Table S1). However, uncertainties associated with dust and woodstove emissions are much higher than most of the other sources, a factor of 10 and 5 respectively (Hanna et al., 1998, 2001; Hu et al., 2014). This uncertainty is driven,

in part, by source variability. This large uncertainty and potential bias is reflected in the large shift in rankings for dust and woodstove source contributions to $PM_{2.5}$. Other biomass burning sources such as lawn waste burning and wildfires have similarly large emissions uncertainties, and likely large temporal variabilities, and their rankings were

5 also significantly decreased. Coal combustion, which includes secondary formation of sulfate, remains in the top three sources for average hybrid $PM_{2.5}$ source contributions at withheld monitors, as its emissions uncertainties are fairly low due to the availability of continuous emission monitoring data.

Secondary formation processes increase the impact of coal combustion, biogenic

10 and livestock emissions relative to their initial primary PM contribution. Coal combustion was ranked 9th, 4th, and 3rd for CMAQ-DDM, CTM-RM, and SH hybrid contributions, respectively. January 2004 primary PM emissions estimates for biogenic and livestock were ranked 33 and 31, respectively. However, CMAQ-DDM, CTM-RM, and SH hybrid contributions ranked both sources significantly higher (biogenic rankings:

15 14, 11, and 9, respectively; livestock rankings: 3, 1, and 1, respectively). Although primary $PM_{2.5}$ emissions from these sources are not large, secondary processes lead to high source contributions. Biogenic sources emit large quantities of volatile organic compounds which go on to form secondary organic aerosols. Livestock emissions, (i.e., gaseous ammonia), react with sulfate, nitrate, and other acids to form ammonium salts.

20 The hybrid CTM-RM method captures and refines impacts from sources that contribute precursors of $PM_{2.5}$.

Refined biomass burning and dust source impacts led to better agreement between simulated and observed concentrations of crustal (Al, Ca, Fe, Si) and biomass burning-derived elements (Cl, K). Original CMAQ-DDM simulations were biased very high for

25 these species compared to observed concentrations. This is due to the apparently high bias in source profile estimates for biomass burning sources, which don't take into account long-range transport and deposition of biomass burning-related PM. Results suggest that due to atmospheric transformation processes, the source profiles are in error for some species, similar to the findings in Balachandran et al. (2013). Ob-

Development of PM$_{2.5}$ source impact spatial fields

C. E. Ivey et al.

Full Screen / Esc

Printer-friendly Version

Interactive Discussion

servational data for some elemental species (Mg, P, Se, V) were highly influenced by measurement limitations (i.e., at or below MDL) and showed the poorest correlation with simulated observations. Additionally, conversion of carbon species between analytical methods, from total optical transmittance to total optical reflectance equivalents,

5 introduced potential bias into concentration comparisons. However, other studies have shown that conversions may overcorrect observations of carbon species (Balachandran et al., 2013).

In summary, the SH method uses observations and modeled concentrations of species to adjust impacts on a source by source basis to provide spatially and tem-
10 porally detailed source impact fields. Figure 5 shows spatial fields of source impacts for soil/crustal material, coal combustion, and other sources, which demonstrates the spatial and temporal completeness of the data that is provided by the SH method. The SH method also captures the impacts of secondary aerosol formation from precursor emission sources. Hybrid adjustment factors can be used to estimate the amount of
15 change in emissions necessary for modeled results to better reflect observations, as emissions are roughly proportional to source impacts for primary sources. Kriging is an effective spatial interpolation method for spatially extending the CTM-RM model and generating spatial fields of adjustment factors. Adjusted CMAQ-DDM spatial fields of source impacts capture prior knowledge of emissions impacts, meteorology, and
20 chemistry. Kriging does not introduce significant error, as the adjusted spatial fields maintain the spatial and temporal variability of the original source impact fields, and this application led to simulated $PM_{2.5}$ mass concentrations being closer to observations. Applying the hybrid model and spatial extension to original CMAQ-DDM source impact estimates also improves simulated estimates of crustal and trace metals.

25 The hybrid model is an effective approach for reducing the error in simulated source impacts through statistical optimization, instead of rerunning CMAQ-DDM which is more computationally expensive. Moreover, the methods presented generate daily, spatially complete fields that can be utilized by atmospheric scientists, air quality managers, and epidemiologists in health-related analyses. In future studies, the model will

Development of PM$_{2.5}$ source impact spatial fields

C. E. Ivey et al.

Title Page

Abstract | Introduction

Conclusions | References

Tables | Figures

◀◀ | ▶▶

◀ | ▶

Back | Close

Full Screen / Esc

Printer-friendly Version

Interactive Discussion

be extended temporally to generate daily, adjusted spatial fields for the continental US for multiple years and to develop improved source profiles for emissions characterization.

The Supplement related to this article is available online at
5 **doi:10.5194/gmdd-8-645-2015-supplement.**

References

Baker, K. R., Simon, H., and Kelly, J. T.: Challenges to modeling "cold pool" meteo-
15 rology associated with high pollution episodes, Environ. Sci. Technol., 45, 7118–7119, doi:10.1021/Es202705v, 2011.
Balachandran, S., Pachon, J. E., Hu, Y. T., Lee, D., Mulholland, J. A., and Russell, A. G.: Ensemble-trained source apportionment of fine particulate matter and method uncertainty analysis, Atmos. Environ., 61, 387–394, doi:10.1016/j.atmosenv.2012.07.031, 2012.
20 Balachandran, S., Chang, H. H., Pachon, J. E., Holmes, H. A., Mulholland, J. A., and Russell, A. G.: Bayesian-based ensemble source apportionment of $PM_{2.5}$, Environ. Sci. Technol., 47, 13511–13518, doi:10.1021/Es4020647, 2013.
Byun, D. and Schere, K. L.: Review of the governing equations, computational algorithms, and other components of the models-3 Community Multiscale Air Quality (CMAQ) modeling sys-
25 tem, Appl. Mech. Rev., 59, 51–77, doi:10.1115/1.2128636, 2006.
Campen, M. J., Nolan, J. P., Schladweiler, M. C. J., Kodavanti, U. P., Evansky, P. A., Costa, D. L., and Watkinson, W. P.: Cardiovascular and thermoregulatory effects of inhaled PM-associated

⏮ | ⏭

◀ | ▶

Back | Close

Full Screen / Esc

Printer-friendly Version

Interactive Discussion

transition metals: a potential interaction between nickel and vanadium sulfate, Toxicol. Sci., 64, 243–252, doi:10.1093/toxsci/64.2.243, 2001.

CEP: Sparse Matrix Operator Kernel Emissions Modeling System (SMOKE) User Manual, Carolina Environmental Program – The University of North Carolina at Chapel Hill, Chapel Hill, NC, 2003.

Chow, J. C., Watson, J. G., Pritchett, L. C., Pierson, W. R., Frazier, C. A., and Purcell, R. G.: The dri thermal optical reflectance carbon analysis system – description, evaluation and applications in United-States air-quality studies, Atmos. Environ. A-Gen., 27, 1185–1201, doi:10.1016/0960-1686(93)90245-T, 1993.

Darrow, L. A., Klein, M., Strickland, M. J., Mulholland, J. A., and Tolbert, P. E.: Ambient air pollution and birth weight in full-term infants in Atlanta, 1994–2004, Environ. Health Persp., 119, 731–737, doi:10.1289/Ehp.1002785, 2011.

Dominici, F., Peng, R. D., Barr, C. D., and Bell, M. L.: Protecting human health from air pollution shifting from a single-pollutant to a multipollutant approach, Epidemiology, 21, 187–194, doi:10.1097/Ede.0b013e3181cc86e8, 2010.

Dunker, A. M.: Efficient calculation of sensitivity coefficients for complex atmospheric models, Atmos. Environ., 15, 1155–1161, doi:10.1016/0004-6981(81)90305-X, 1981.

Dunker, A. M.: The decoupled direct method for calculating sensitivity coefficients in chemical-kinetics, J. Chem. Phys., 81, 2385–2393, doi:10.1063/1.447938, 1984.

Fletcher, R.: Practical Methods of Optimization, John Wiley and Sons, 1987.

Gill, P. E., Murray, W., and Wright, M. H.: Practical Optimization, Academic Press, London, 1981.

Grell, G., Dudhia, J., and Stauffer, D.: A Description of the Fifth-Generation Penn State/NCAR Mesoscale Model (MM5), NCAR Technical Note: NCAR/TN-398+STRNCAR/TN 398+STR, 1994.

Hanna, S. R., Chang, J. C., and Fernau, M. E.: Monte Carlo estimates of uncertainties in predictions by a photochemical grid model (UAM-IV) due to uncertainties in input variables, Atmos. Environ., 32, 3619–3628, doi:10.1016/S1352-2310(97)00419-6, 1998.

Hanna, S. R., Lu, Z. G., Frey, H. C., Wheeler, N., Vukovich, J., Arunachalam, S., Fernau, M., and Hansen, D. A.: Uncertainties in predicted ozone concentrations due to input uncertainties for the UAM-V photochemical grid model applied to the July 1995 OTAG domain, Atmos. Environ., 35, 891–903, doi:10.1016/S1352-2310(00)00367-8, 2001.

Hansen, D. A., Edgerton, E. S., Hartsell, B. E., Jansen, J. J., Kandasamy, N., Hidy, G. M., and Blanchard, C. L.: The southeastern aerosol research and characterization study: Part 1-overview, JAPCA J. Air Waste Ma., 53, 1460–1471, 2003.

Hansen, D. A., Edgerton, E., Hartsell, B., Jansen, J., Burge, H., Koutrakis, P., Rogers, C., Suh, H., Chow, J., Zielinska, B., McMurry, P., Mulholland, J., Russell, A., and Rasmussen, R.: Air quality measurements for the aerosol research and inhalation epidemiology study, JAPCA J. Air Waste Ma., 56, 1445–1458, 2006.

Hu, Y., Balachandran, S., Pachon, J. E., Baek, J., Ivey, C., Holmes, H., Odman, M. T., Mulholland, J. A., and Russell, A. G.: Fine particulate matter source apportionment using a hybrid chemical transport and receptor model approach, Atmos. Chem. Phys., 14, 5415–5431, doi:10.5194/acp-14-5415-2014, 2014.

Laden, F., Neas, L. M., Dockery, D. W., and Schwartz, J.: Association of fine particulate matter from different sources with daily mortality in six US cities, Environ. Health Persp., 108, 941–947, doi:10.1289/Ehp.00108941, 2000.

Lim, S. S., Vos, T., Flaxman, A. D., Danaei, G., Shibuya, K., Adair-Rohani, H., Amann, M., Anderson, H. R., Andrews, K. G., Aryee, M., Atkinson, C., Bacchus, L. J., Bahalim, A. N., Balakrishnan, K., Balmes, J., Barker-Collo, S., Baxter, A., Bell, M. L., Blore, J. D., Blyth, F., Bonner, C., Borges, G., Bourne, R., Boussinesq, M., Brauer, M., Brooks, P., Bruce, N. G., Brunekreef, B., Bryan-Hancock, C., Bucello, C., Buchbinder, R., Bull, F., Burnett, R. T., Byers, T. E., Calabria, B., Carapetis, J., Carnahan, E., Chafe, Z., Charlson, F., Chen, H. L., Chen, J. S., Cheng, A. T. A., Child, J. C., Cohen, A., Colson, K. E., Cowie, B. C., Darby, S., Darling, S., Davis, A., Degenhardt, L., Dentener, F., Des Jarlais, D. C., Devries, K., Dherani, M., Ding, E. L., Dorsey, E. R., Driscoll, T., Edmond, K., Ali, S. E., Engell, R. E., Erwin, P. J., Fahimi, S., Falder, G., Farzadfar, F., Ferrari, A., Finucane, M. M., Flaxman, S., Fowkes, F. G. R., Freedman, G., Freeman, M. K., Gakidou, E., Ghosh, S., Giovannucci, E., Gmel, G., Graham, K., Grainger, R., Grant, B., Gunnell, D., Gutierrez, H. R., Hall, W., Hoek, H. W., Hogan, A., Hosgood, H. D., Hoy, D., Hu, H., Hubbell, B. J., Hutchings, S. J., Ibeanusi, S. E., Jacklyn, G. L., Jasrasaria, R., Jonas, J. B., Kan, H. D., Kanis, J. A., Kassebaum, N., Kawakami, N., Khang, Y. H., Khatibzadeh, S., Khoo, J. P., Kok, C., Laden, F., Lalloo, R., Lan, Q., Lathlean, T., Leasher, J. L., Leigh, J., Li, Y., Lin, J. K., Lipshultz, S. E., London, S., Lozano, R., Lu, Y., Mak, J., Malekzadeh, R., Mallinger, L., Marcenes, W., March, L., Marks, R., Martin, R., McGale, P., McGrath, J., Mehta, S., Mensah, G. A., Merriman, T. R., Micha, R., Michaud, C., Mishra, V., Hanafiah, K. M., Mok-

Development of PM$_{2.5}$ source impact spatial fields

C. E. Ivey et al.

Title Page

Abstract	Introduction
Conclusions	References
Tables	Figures

|◄   ►|

◄   ►

| Back | Close |

Full Screen / Esc

Printer-friendly Version

Interactive Discussion

dad, A. A., Morawska, L., Mozaffarian, D., Murphy, T., Naghavi, M., Neal, B., Nelson, P. K., Nolla, J. M., Norman, R., Olives, C., Omer, S. B., Orchard, J., Osborne, R., Ostro, B., Page, A., Pandey, K. D., Parry, C. D. H., Passmore, E., Patra, J., Pearce, N., Pelizzari, P. M., Petzold, M., Phillips, M. R., Pope, D., Pope, C. A., Powles, J., Rao, M., Razavi, H., Rehfuess, E. A., Rehm, J. T., Ritz, B., Rivara, F. P., Roberts, T., Robinson, C., Rodriguez-Portales, J. A., Romieu, I., Room, R., Rosenfeld, L. C., Roy, A., Rushton, L., Salomon, J. A., Sampson, U., Sanchez-Riera, L., Sanman, E., Sapkota, A., Seedat, S., Shi, P. L., Shield, K., Shivakoti, R., Singh, G. M., Sleet, D. A., Smith, E., Smith, K. R., Stapelberg, N. J. C., Steenland, K., Stockl, H., Stovner, L. J., Straif, K., Straney, L., Thurston, G. D., Tran, J. H., Van Dingenen, R., van Donkelaar, A., Veerman, J. L., Vijayakumar, L., Weintraub, R., Weissman, M. M., White, R. A., Whiteford, H., Wiersma, S. T., Wilkinson, J. D., Williams, H. C., Williams, W., Wilson, N., Woolf, A. D., Yip, P., Zielinski, J. M., Lopez, A. D., Murray, C. J. L., and Ezzati, M.: A comparative risk assessment of burden of disease and injury attributable to 67 risk factors and risk factor clusters in 21 regions, 1990–2010: a systematic analysis for the Global Burden of Disease Study 2010, Lancet, 380, 2224–2260, 2012.

Napelenok, S. L., Cohan, D. S., Hu, Y. T., and Russell, A. G.: Decoupled direct 3D sensitivity analysis for particulate matter (DDM-3D/PM), Atmos. Environ., 40, 6112–6121, doi:10.1016/j.atmosenv.2006.05.039, 2006.

Oberdorster, G., Oberdorster, E., and Oberdorster, J.: Nanotoxicology: an emerging discipline evolving from studies of ultrafine particles, Environ. Health Persp., 113, 823–839, doi:10.1289/Ehp.7339, 2005.

Peel, J. L., Klein, M., Flanders, W. D., Mulholland, J. A., Freed, G., and Tolbert, P. E.: Ambient air pollution and apnea and bradycardia in high-risk infants on home monitors, Environ. Health Persp., 119, 1321–1327, doi:10.1289/Ehp.1002739, 2011.

Peters, A., Wichmann, H. E., Tuch, T., Heinrich, J., and Heyder, J.: Respiratory effects are associated with the number of ultrafine particles, Am. J. Resp. Crit. Care, 155, 1376–1383, 1997.

Pleim, J. E. and Xiu, A.: Development and testing of a surface flux and planetary boundary-layer model for application in mesoscale models, J. Appl. Meteorol., 34, 16–32, doi:10.1175/1520-0450-34.1.16, 1995.

Pope, C. A., Burnett, R. T., Thun, M. J., Calle, E. E., Krewski, D., Ito, K., and Thurston, G. D.: Lung cancer, cardiopulmonary mortality, and long-term exposure to fine particulate air pollution, JAMA-J. Am. Med. Assoc., 287, 1132–1141, doi:10.1001/jama.287.9.1132, 2002.

Reff, A., Bhave, P. V., Simon, H., Pace, T. G., Pouliot, G. A., Mobley, J. D., and Houyoux, M.: Emissions inventory of PM$_{2.5}$ trace elements across the United States, Environ. Sci. Technol., 43, 5790–5796, doi:10.1021/Es802930x, 2009.

Samet, J. M., Dominici, F., Curriero, F. C., Coursac, I., and Zeger, S. L.: Fine particulate air pollution and mortality in 20 US cities, 1987–1994., New Engl. J. Med., 343, 1742–1749, doi:10.1056/Nejm200012143432401, 2000.

Sarnat, J. A., Marmur, A., Klein, M., Kim, E., Russell, A. G., Sarnat, S. E., Mulholland, J. A., Hopke, P. K., and Tolbert, P. E.: Fine particle sources and cardiorespiratory morbidity: an application of chemical mass balance and factor analytical source-apportionment methods, Environ. Health Persp., 116, 459–466, doi:10.1289/Ehp.10873, 2008.

Seigneur, C., Pun, B., Pai, P., Louis, J. F., Solomon, P., Emery, C., Morris, R., Zahniser, M., Worsnop, D., Koutrakis, P., White, W., and Tombach, I.: Guidance for the performance evaluation of three-dimensional air quality modeling systems for particulate matter and visibility, JAPCA J. Air Waste Ma., 50, 588–599, 2000.

Thurston, G. D., Ito, K., Mar, T., Christensen, W. F., Eatough, D. J., Henry, R. C., Kim, E., Laden, F., Lall, R., Larson, T. V., Liu, H., Neas, L., Pinto, J., Stolzel, M., Suh, H., and Hopke, P. K.: Workgroup report: workshop on source apportionment of particulate matter health effects – intercomparison of results and implications, Environ. Health Persp., 113, 1768–1774, doi:10.1289/Ehp.7989, 2005.

Tolbert, P. E., Klein, M., Peel, J. L., Sarnat, S. E., and Sarnat, J. A.: Multipollutant modeling issues in a study of ambient air quality and emergency department visits in Atlanta, J. Expo. Sci. Env. Epid., 17, S29–S35, doi:10.1038/sj.jes.7500625, 2007.

Wang, X. B., Ding, H., Ryan, L., and Xu, X. P.: Association between air pollution and low birth weight: a community-based study, Environ. Health Persp., 105, 514–520, doi:10.1289/Ehp.97105514, 1997.

Watson, J. G., Cooper, J. A., and Huntzicker, J. J.: The effective variance weighting for least-squares calculations applied to the mass balance receptor model, Atmos. Environ., 18, 1347–1355, doi:10.1016/0004-6981(84)90043-X, 1984.

Xiu, A. J. and Pleim, J. E.: Development of a land surface model. Part I: Application in a mesoscale meteorological model, J. Appl. Meteorol., 40, 192–209, doi:10.1175/1520-0450(2001)040<0192:Doalsm>2.0.Co;2, 2001.

Table 1. Source category abbreviations with average CMAQ-DDM, CTM-RM, and SH (spatial hybrid) source contributions to PM$_{2.5}$ concentrations for withheld CSN monitors ($N = 75$ monitors) for January 2004. Note: All averages and SDs are expressed in $\mu g\,m^{-3}$. Average total mass over withheld monitors for observations, CMAQ-DDM, CTM-RM, and SH was 11.7($\pm$8.3), 16.3($\pm$11), 8.59($\pm$4.7), and 9.2($\pm$5.7) $\mu g\,m^{-3}$. NR = Nonroad, CM = Combustion.

Source Categories	Abbreviation	CMAQ-DDM			CTM-RM			SH Hybrid		
		Avg.	St. Dev.	Rank	Avg.	St. Dev.	Rank	Avg.	St. Dev.	Rank
Agricultural Burning	AGRIBURN	0.0040	0.003	25	0.0016	0.011	26	0.0012	0.0052	28
Aircraft Emissions	AIRCRAFT	0.0038	0.013	26	0.0037	0.013	25	0.0038	0.013	25
Biogenic Emissions	BIOGENIC	0.074	0.22	14	0.069	0.22	11	0.074	0.22	9
Coal CM	COALCMB	0.16	0.39	9	0.15	0.38	4	0.15	0.38	3
Diesel CM.	DIESELCM	0.00060	0.0017	30	0.0006	0.0017	30	0.0006	0.0017	30
Dust	DUST	0.36	0.095	2	0.061	0.22	13	0.048	0.12	14
Fuel Oil CM	FUELOILC	0.14	0.54	12	0.14	0.62	6	0.14	0.63	5
Livestock Emissions	LIVEST2	0.31	0.89	3	0.31	0.85	1	0.31	0.88	1
Liquid Petroleum Gas CM	LPGCMB	0.0043	0.013	24	0.0043	0.013	24	0.0043	0.013	24
Lawn Waste Burning	LWASTEBU	0.10	0.032	13	0.018	0.067	21	0.010	0.026	22
Metal Processing	METALPR	0.18	0.16	7	0.12	0.70	7	0.064	0.22	12
Meat Cooking	MEATCOOK	0.034	0.089	19	0.034	0.10	16	0.032	0.10	17
Mexican CM	MEXCMB_M	0.00070	0.0028	29	0.0007	0.0028	29	0.0007	0.0028	29
Mineral Processing	MINERALP	0.030	0.062	21	0.026	0.075	19	0.024	0.076	19
Natural Gas CM	NAGASCMB	0.17	0.21	8	0.11	0.36	8	0.078	0.20	8
NR Diesel CM	NRDIESEL	0.14	0.48	11	0.14	0.73	5	0.14	0.73	4
NR Fuel Oil CM	NRFUELOI	0.010	0.036	23	0.010	0.041	23	0.010	0.039	23
NR Gasoline CM	NRGASOL	0.063	0.22	16	0.061	0.23	14	0.064	0.23	13
NR Liquid Petroleum Gas CM	NRLPG	0.0014	0.0056	28	0.0014	0.0056	27	0.0014	0.0056	26
NR Natural Gas CM	NRNAGAS	0.0005	0.0014	31	0.0005	0.0014	31	0.0005	0.0014	31
Other NR Sources	NROTHERS	0.0005	0.0012	32	0.0005	0.0012	32	0.0005	0.0012	32
Open Fires	OPENFIRE	0.15	0.099	10	0.021	0.11	20	0.017	0.10	20
Onroad Diesel CM	ORDIESEL	0.070	0.17	15	0.066	0.19	12	0.068	0.19	11
Onroad Gasoline CM	ORGASOL	0.27	0.60	4	0.20	0.54	2	0.24	0.62	2
Other CM Sources	OTHERCMB	0.040	0.072	18	0.029	0.14	18	0.026	0.11	18
Other PM Sources	OTHERS2	0.18	0.22	6	0.10	0.28	9	0.10	0.28	7
Prescribed Burning	PRESCRBU	0.032	0.054	20	0.031	0.24	17	0.032	0.24	16
Railroad Emissions	RAILROAD	0.013	0.046	22	0.013	0.046	22	0.013	0.045	21
Seasalt	SEASALT	0.0001	0.0005	33	0.0001	0.0005	33	0.00	0.0	33
Solvent Emissions	SOLVENT	0.051	0.094	17	0.044	0.14	15	0.040	0.13	15
Wildfires	WILDFIRE	0.0018	0.0034	27	0.0012	0.0033	28	0.0013	0.00	27
Woodfuel Burning	WOODFUEL	0.22	0.28	5	0.20	1.3	3	0.12	0.90	6
Woodstoves	WOODSTOV	0.62	0.44	1	0.083	0.29	10	0.069	0.28	10
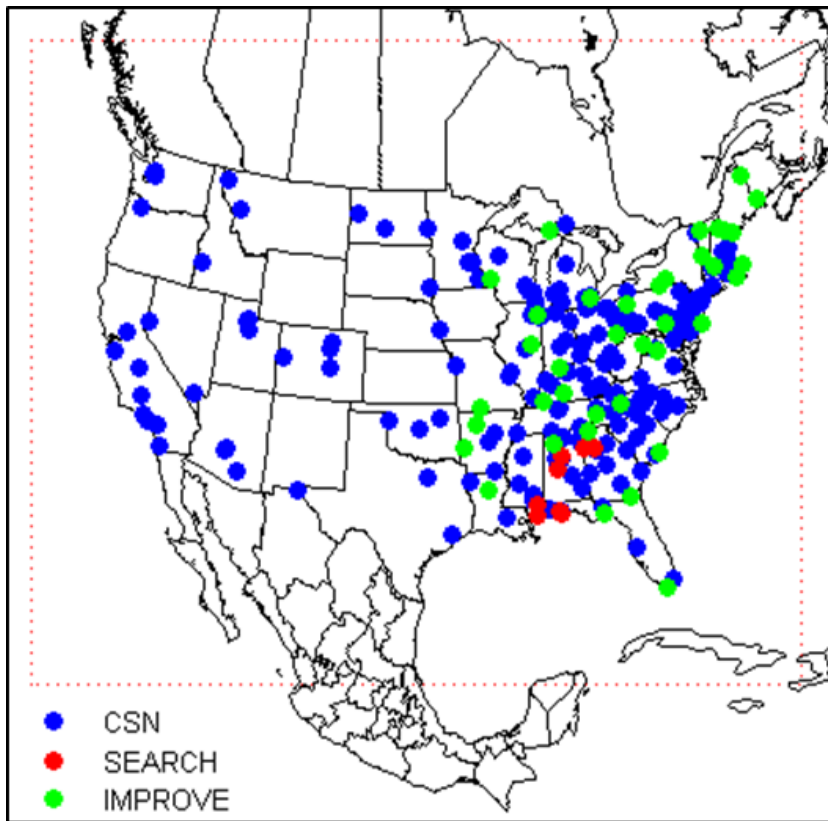
Figure 1. Modeling domain (dotted, red line) and CSN, SEARCH, and IMPROVE monitors used for model development, application, and evaluation.

Figure 2. Spatial fields of kriged adjustment factors (R_j^{SH}) for dust, on-road diesel combustion, on-road gasoline combustion, and woodstove sources for 4 January 2004. Adjustment factors at CSN monitors (denoted by circles) were generated using hybrid (CTM-RM) source apportionment. Note that each figure has a different scale.

Title Page

Abstract | Introduction

Conclusions | References

Tables | Figures

|◀ | ▶|

◀ | ▶

Back | Close

Full Screen / Esc

Printer-friendly Version

Interactive Discussion
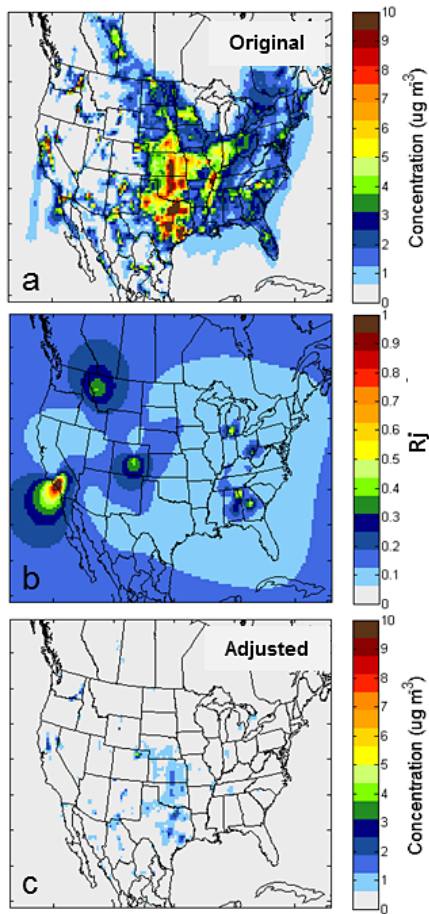
Figure 3. Hybrid-kriging adjustment of the dust impacts on PM$_{2.5}$ on 22 January 2004. **(a)** Original CMAQ-DDM simulation of dust source impacts. **(b)** Spatial field of hybrid adjustment factors for dust (R_j^{SH}). **(c)** Adjusted spatial field of dust source impacts.

Title Page

Abstract | Introduction

Conclusions | References

Tables | Figures

|◄ | ►|

◄ | ►

Back | Close

Full Screen / Esc

Printer-friendly Version

Interactive Discussion

Full Screen / Esc

Printer-friendly Version

Interactive Discussion

Figure 4. CTM-RM vs. Spatial Hybrid adjustment factors for withheld CSN monitors. Regression statistics: intercept, $\alpha = 0.14 \pm 0.02$; slope, $\beta = 0.84 \pm 0.02$; and correlation coefficient, $r = 0.89$.
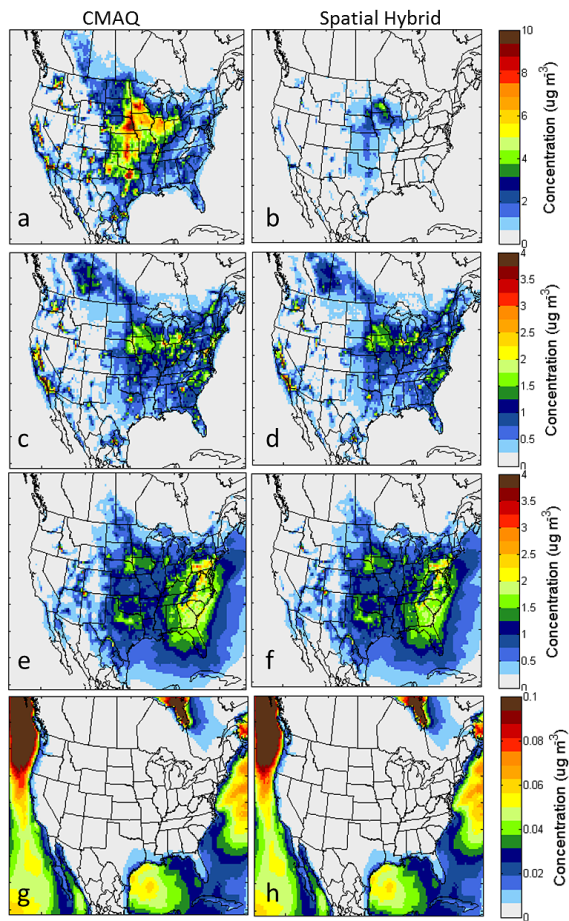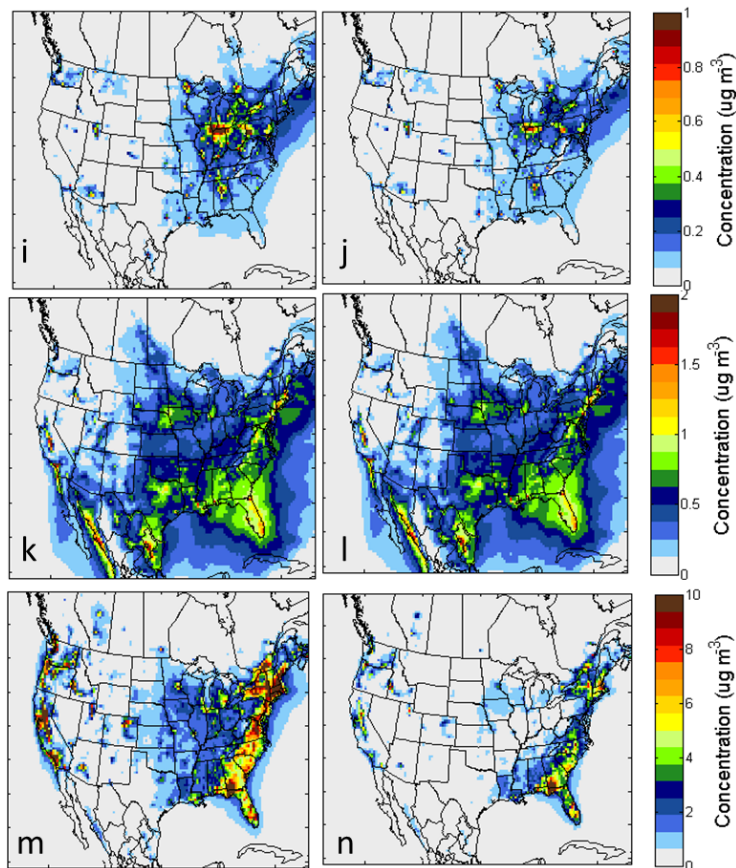
Figure 5.

Figure 5. Average CMAQ-DDM and spatial hybrid source impacts on PM$_{2.5}$ for observation days in January 2004 for seven source categories. Impact of **(a, b)** soil/crustal material, **(c, d)** traffic-related sources, **(e, f)** coal combustion, **(g, h)** sea salt aerosol, **(i, j)** metals-related sources, **(k, l)** fuel oil combustion, and **(m, n)** biomass burning.